

Toward the Design and Synthesis of Lithium-Ion Intercalation into a Coordination $\pi-\pi$ Framework Host

Lih-Wen Huang,^[b] Chia-Jung Yang,^[a] and Kuan-Jiuh Lin*^[a]

Dedicated to Professor Sunney I. Chan on the occasion of his 65th birthday

Abstract: A π -stacked coordination solid, $[[[(VO)_2(OH)_2(C_4O_4)(phen)_2] \cdot H_2O]_n]$ (**1**: phen = phenanthroline), was synthesized by hydrothermal methods and structurally characterized by X-ray single-crystal diffraction. The structure of **1** adopts a neutral open framework in which channeling apertures and windows are surrounded by four oxovanadyl dimers, two squarates, and two pairs of $\pi-\pi$ interactions of phenanthroline

groups; the dimensions of the windows are about $5.38 \times 7.55 \text{ \AA}$ along the *c* axis. Surprisingly, the porous framework with hydrophilic and hydrophobic characteristics was thermally stable up to 250°C ,

Keywords: hydrothermal synthesis • microporous materials • squaric acid • supramolecular chemistry • vanadium

as indicated from powder X-ray diffraction patterns and thermogravimetric analysis. Further investigation of lithium-ion intercalation into the channel matrix of **1** was conformed by ^7Li NMR spectroscopy and cyclic voltammetry measurements. The present case represents the first example of a porous coordination solid that possesses polar channels capable of mediating lithium-ion insertion.

Introduction

Insertion of electron donors such Li^+ or H^+ into a host lattice is technically important as electrodes for solid-state batteries and in electrochromic devices.^[1–3] The creation of microporous structures as lithium-ion insertion materials is an attractive research field for the storage and transport of lithium ions.^[4–6] In addition to graphite, a wide variety of inorganic solids, such as layered metal oxides and zeolites, have been investigated in great detail.^[7–9] Recently, the world of crystalline porous materials has emerged as an exciting area of supramolecular chemistry.^[10, 11] The discovery of new families of porous coordination materials has raised hopes that such materials could be tailored for new applications, for example, in catalysis, separation, ion-exchange processes, sensors, and nano-technology.^[12, 13] Coordination polymers constructed from transition metals and bridging organic ligands have afforded new types of robust crystals with high degree of porosity.^[14–17] However, the goal in the research for porous coordination framework is not simply to mimic

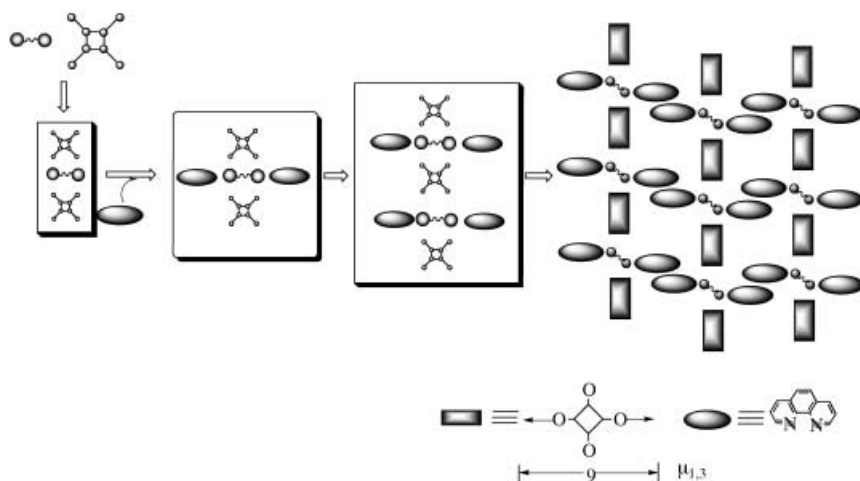
inorganic materials, such as graphite and metal oxides, and the reports of lithium-ion intercalation into such coordination hosts are exceedingly rare or lacking. The correspondence study has been hampered by some inherent properties, such as low thermal stability and low crystal energy in organic ligands that act as structural buttresses. Therefore, a rational synthetic strategy is a key point for the creation of porous coordination polymers that intercalate lithium ions. We propose that the following basic requirements are necessary for a candidate lithium-ion-insertion material:

- 1) A polar environment in cavities that can be filled with ionic species to increase the crystal energy,^[18] affording large free energy of intercalation reactions ($A^+ + e^- + [ML_n] \rightarrow [AML_n]$, $\Delta G = -nFe$: A, M, and L are alkali, transition metal, and organic ligands, respectively).
- 2) Oxygen-rich metal centers, affording redox intercalation conditions.
- 3) Robust host and suitable size matrix, affording a pathway for facile lithium-ion diffusion.

Encouraged by our success in using polyfunctional squarate ligands as a rigid tether for the construction of extended solids under hydrothermal conditions,^[17] we have turned our attention to introduce noncovalent $\pi-\pi$ interactions in the metal–squarate phases to generate new classes of coordination zeolites with hydrophilic and hydrophobic void characteristics.^[19] By adopting this strategy and exploiting the efficiency of the hydrothermal synthetic technique, we have now been able to prepare and isolate new types of coordination $\pi-\pi$ networks constructed from bimetal–squarate phases incor-

[a] Prof. Dr K.-J. Lin, C.-J. Yang
Department of Chemistry
National Chung-Hsing University
Taichung, 402 Taiwan (Republic Of China)
Fax: (+ 886)-4-22862547
E-mail: kjlin@dragon.nchu.edu.tw

[b] L.-W. Huang
Institute of Chemistry
Academia Sinica, Taipei (Taiwan)



Scheme 1. Schematic representation of the coordination π - π networks constructed from bimetal-squarate phases incorporating phen molecules.

porating organic molecules (Scheme 1). Herein we describe a novel coordination polymer, $[[[(VO)_2(OH)_2(C_4O_4)(phen)_2] \cdot H_2O)_n]$ (**1**: phen = phenanthroline) that adopts a neutral open framework with a two-dimensional, intersecting system of channels containing disordered water molecules. These disordered water molecules can be driven out of the structure without deformation of the crystalline. Moreover, the key features of compound **1** rest on the reducible V^{IV} centers and polar cavities or channels. Such benefits have prompted us to study the feasibility of using the novelty of the channel structure of **1** as a lithium-ion insertion material.

Results and Discussion

Synthesis and characterizations of 1: Crystals of **1** were grown from a mixture of V_2O_5 , $H_2C_4O_4$, phen, and H_2O in the molar ratio 2:2:1:888 kept at 200°C for 96 h. The hydrothermal

Abstract in Chinese: 利用水熱合成法與 x-光單晶繞射儀的結構鑑定，我們已經成功的合成出利用配位共價鍵與 π - π 作用力所堆積而成的網狀配位聚合物，結構分子式為 $[(VO)_2(OH)_2(C_4H_4)(phen)_2 \cdot H_2O)_n]$ 。此晶體結構同時具有中性且開放的孔道，大小約 5.38×7.55 Å。在它的孔道中有一熱振動範圍極大、性質不穩定的水分子，並且經由 x-光粉末繞射儀與熱重分析儀(TGA)的研究結果，發現水分子可以自由進出此孔道，熱穩定性可以到 250°C 。另外，這個由 π - π 作用力所架構出來的孔洞結構還具有親水性與疏水性的雙重吸附特性。更重要的是，藉由鋰電池的原理機制，並經由 Li-NMR 與循環伏安法(CV)的實驗證明，我們已成功將鋰離子嵌入此化合物的通道中。這將開啟有機鋰電池及鋰離子感測器在超分子材料的應用範疇。本文所介紹的化合物是孔洞配位聚合物中，第一個同時具有讓鋰離子嵌入特性的研究報告。

synthesis provides an opportunity to obtain high yield (74 %) and was highly reproducible. Compound **1** was formulated from elemental analysis and structurally characterized by single-crystal X-ray diffraction. The X-ray structural analysis of **1** reveals an extended structure composed of the building block shown in Figure 1. The dimeric octahedral oxovanadyl centers ($V^{IV}=\text{O}$, $d_{V=\text{O}}=1.596(2)$ Å) are bridged by two hydroxides,^[20] and each metal is coordinated by a phen ligand and linked by squarate anions in a $\mu_{1,3}$ -bridging mode. The

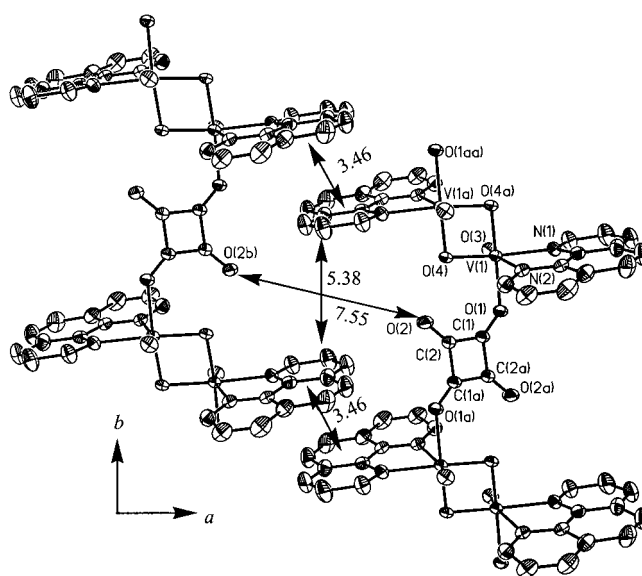


Figure 1. An ORTEP plot of a section of two adjacent infinite chains (50 % probability ellipsoid; hydrogen atoms are omitted for clarity), showing the architecture of an open window formed through coordination bonds and noncovalent π - π interactions. Selected bond lengths [Å] and angles [$^\circ$]: V(1)-N(1) 2.136(3), V(1)-N(2) 2.351(3), V(1)-O(1) 2.051(2), V(1)-O(3) 1.596(2), V(1)-O(4) 1.971(2), V(1)-O(4a) 1.955(2), V(1)-V(1a) 3.036(1), C(1)-O(1) 1.253(4), C(2)-O(2) 1.242(4), C(1)-C(2) 1.467(2), C(1)-C(2a) 1.480(2); O(3)-V(1)-O(4a) 105.3(1), O(3)-V(1)-O(4) 103.0(1), O(4)-V(1)-O(4a) 78.7(1), O(1)-V(1)-O(3) 95.6(1), O(1)-V(1)-O(4a) 93.6(1), O(1)-C(1)-C(2) 130.9(3), C(2)-C(1)-C(2a) 91.0(3).

$\{O=V(\mu\text{-OH})_2V=O\}$ core has been observed in our previous work^[17] and also elsewhere^[21]. The bond-valence sum (BVS) of vanadium is 3.98.^[22] Moreover, compound **1** has a magnetic moment of $1.63 \mu_B$ at 300 K, which is comparable to those in the oxovanadyl (VO^{2+}) complexes.^[21] The structure of **1** may be described as one-dimensional inorganic infinite chains, $\{-C_4O_4-(VO(OH)_2-C_4O_4)-\}_n$, which incorporate the phen ligands. These incorporated phen rings, however, play an important role in the construction of a π -stacked layer structure between adjacent crystallographically symmetry-related chains. Within the layer there are “rectangular”

windows with dimensions of about $5.38 \times 7.55 \text{ \AA}$ (interplane π distances and $\text{O} \cdots \text{O}$ distances, respectively), each of which is surrounded by four oxovanadyl dimers, two $\mu_{1,3}$ -squate anions, and two pairs of π -groups of phen rings. Furthermore, adjacent layers are stacked on top of each other along the c axis and are glued by cooperative $\text{CH} \cdots \pi$ interactions. This sort of π - π networks gives rise to two types of infinite microchannels. The main channels are those that run along the c axis as a consequence of the stacking of the rectangular windows (Figure 2a). The other small channels enclosed by phen moieties run along the b -axis (Figure 2b).

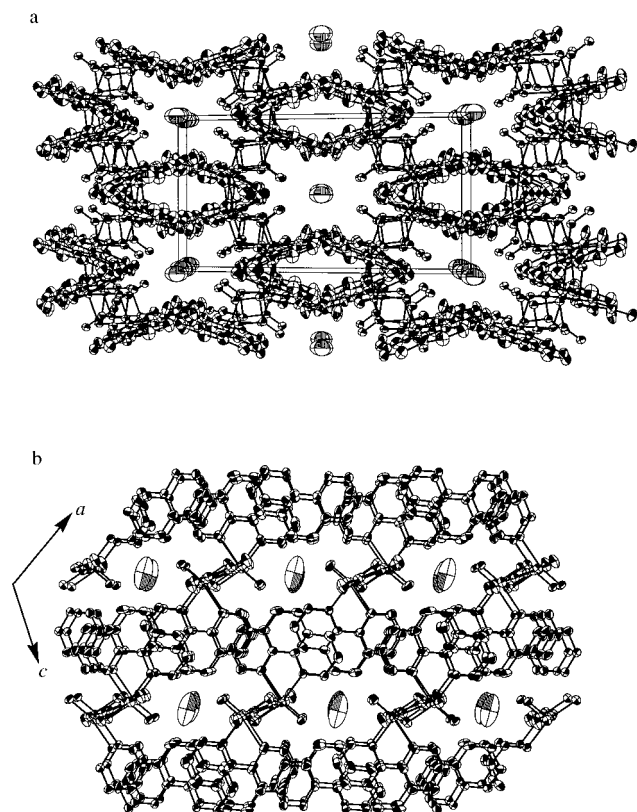


Figure 2. Perspective views of crystal structure along a) the c axis and b) the b axis, showing the disordered water molecules located at the intersection of the channels.

An interesting feature of **1** is the presence of disordered water molecules trapped at the intersection of channels. In order to examine the thermal stability of this porous network, thermogravimetric analysis (TGA) and measurements of powder X-ray diffraction patterns (PXRD) were carried out. The TGA reveals that the water guests are liberated below 150°C , a weight loss of 2.7% consistent with one H_2O per formula unit. No weight loss was observed in the temperature range 150 – 290°C . For the purpose of examining the porous functionality of **1**, desorption–adsorption water cycling study between 40 – 150°C was conducted. TGA traces for heating and cooling scans, measured with a rate of 2°Cmin^{-1} , are given in Figure 3. It reveals a reversible water sorption cycle in the channels of **1**. Moreover, the PXRD patterns and a pattern simulated on the basis of the single-

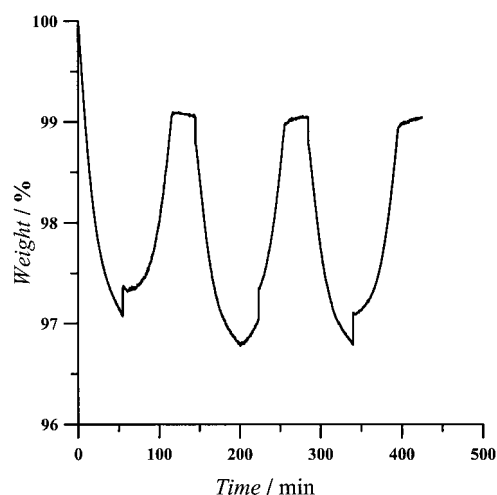


Figure 3. TGA profile of the water reversible desorption–adsorption study on **1**. The sample was initially heated to 150°C at 2°Cmin^{-1} in a dry N_2 flux. The sample was then cooled to 40°C , maintained at 40°C for 0.5 h in a H_2O vapor/ N_2 carrier; a gradual weight increase was observed that reached $\sim 2 \text{ wt } \%$. Subsequently, repeated heating-and-cooling processes were conducted between 40 – 150°C , revealing a reversible water desorption–adsorption cycle.

crystal structure are presented in Figure 4. The positions of the diffraction peaks of **1** (Figure 4b) compared well with those in the calculated one (Figure 4a), indicating that the sample of **1** is a pure phase. Furthermore, after the sample of **1** had been heated at 250°C for four hours, the diffraction peaks remained unchanged relative to unheated sample of **1** (Figure 4c). The good agreement between PXRD patterns demonstrates that the porous framework was retained even after the partial loss of water molecules. Therefore, we conclude that the π - π buttresses are robust enough to sustain such an open space in the crystal. Owing to the stability of the

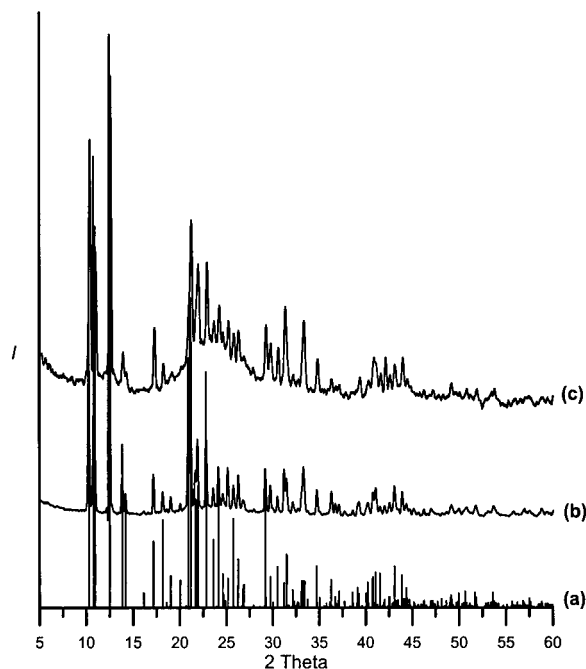


Figure 4. X-ray powder patterns a) calculated from single crystal structure, b) recorded at room temperature, and c) recorded after the treatment by heating at 250°C for four hours.

porous framework, compound **1** can be considered a “zeolite analogue” material with hydrophobic (phen groups) and hydrophilic (four oxygen atoms from the pendant groups of the squarates pointed toward the channels, see Figure 2) moieties covering the walls of the channels. The size of the channels is similar to those observed in some zeolite molecular sieves, such as, analcime (2.2 Å) in which water (kinetic diameter is 2.8 Å) is known to penetrate and diffuse into the channels.^[23] Having the reducible V^{IV} center as well as the functionalized voids that would benefit the bonding interactions of Li⁺⋯O and Li⁺⋯π, the present of vacant channels of **1** afford potential sites for lithium-ion intercalation.

Lithium-ion intercalation of 1: Investigation of lithium-ion intercalation into channel matrix of **1** may provide interesting materials, for example, cathode materials in solid-state batteries. Scheme 2 illustrates that compound **1** could be intercalated with lithium reagents to give reduced phases, **Li·1**. Both cations and electrons transferred to the host possess considerable mobility in **Li·1** phases, rendering them mixed ionic–electronic conductors. Many examples of topochemical lithium-ion incorporation into inorganic framework materials have been reported.^[9, 24] Among these synthetic techniques, a lithiating reagent such as *n*-butyllithium can be used for the formation of reduced phases and to provide efficient lithium-ion intercalation ($x\text{C}_4\text{H}_9\text{Li} + \mathbf{1} \rightarrow \mathbf{Li}\cdot\mathbf{1} + \frac{x}{2}\text{C}_8\text{H}_{18} + x\text{H}_2\text{O}$). The best known example of alkali metal ion intercalation is that of the lithium ion into TiS₂ to give Li_xTiS₂.^[24] Lithium-ion intercalation of **1** using *n*-butyllithium was carried out in a similar fashion. Crystals of **1** change from orange to deep black upon lithium-ion intercalation. The presence of Li⁺ in **Li·1** was determined by ⁷Li NMR spectroscopy, as a signal was observed at $\delta = 0.072$ relative to that of free LiNO₃. Moreover, IR studies offer further information on the possible interactions of Li⁺⋯O and Li⁺⋯π in **Li·1**. The FTIR spectrum of **1** exhibits two broad envelopes of features at around 1450–1650 and 2800–3000 cm^{−1}, due to the hydrogen-bonding between squarate and free lattice water molecules and the π–π networks between phen molecules. The broad features were almost totally removed due to the interactions of Li⁺⋯O and Li⁺⋯π in **Li·1**, thus giving more intense and relatively sharp features at about 1377, 1420, 1470, 1513 $\nu(\text{C}=\text{C}, \text{C}=\text{O})$ and 2853, 2924,

2955 cm^{−1} $\nu(\text{C}-\text{H})$. It is noteworthy that PXRD pattern of **Li·1** shows that the positions of the most intense lines remain unchanged relative to the simulated pattern based of the single-crystal data of **1**; this indicates that the channel crystallinity was retained in the course of intercalation. Furthermore, we want to exam whether the oxidation number of oxovanadyl centers decreases upon intercalating lithium ions into **1**. By employing cyclic voltammetry (CV), the oxidation numbers of vanadium ions were deduced (Figure 5). The voltammogram recorded for **Li·1** exhibits

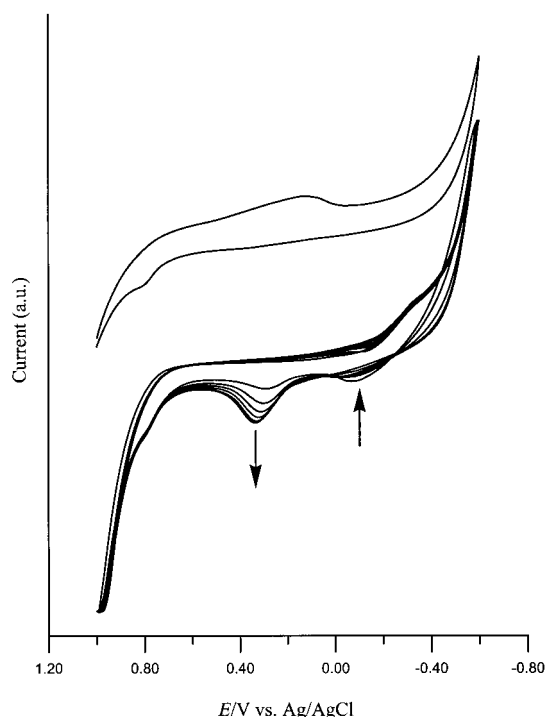
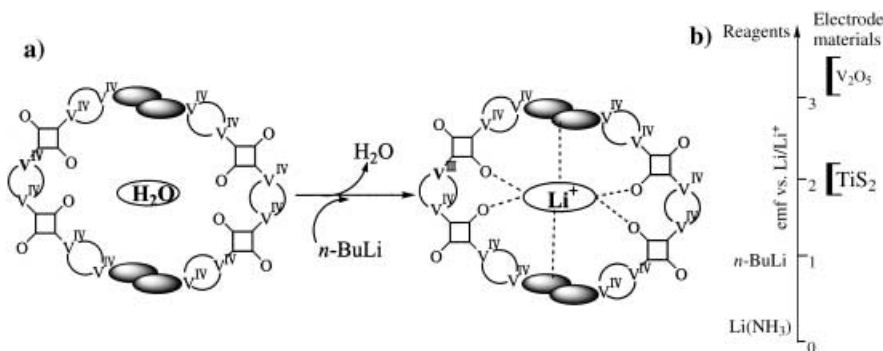


Figure 5. Cyclic voltammogram of **1** (upper) and **Li·1** (lower) in CH₃COOH at a scan rate of 100 mV s^{−1}. Arrows indicate the decrease in intensity of the V^{II}/V^{III} (−0.19 V) band, and the increase in intensity of the V^{III}/V^{IV} (0.33 V) band in the course of oxidation scans.

three peaks at 0.8, 0.33, and −0.19 V versus Ag⁺/AgCl in the course of oxidation scans. This observation has been attributed the vanadium ions in **Li·1** being in mixed-valence states of +4, +3, and +2, that is, the reduction of V^{IV} to V^{II} and V^{III} is accompanied by lithium-ion intercalation of **1**. Moreover, correlation between the V^{II}/V^{III} and V^{III}/V^{IV} oxidative bands is

clearly seen (indicated by the arrows); during the oxidation scan the intensity of V^{II}/V^{III} band decreases, whereas that of V^{III}/V^{IV} band increases. As anticipated, compound **1** can be intercalated with lithium ions to give the reduced vanadium phase, for which the solid-state structure remains unchanged. Further characterizations including ionic conductivity and reversible cycling are in progress.



Scheme 2. a) Schematic representation of the lithium-ion intercalation reaction of **1** ($x\text{C}_4\text{H}_9\text{Li} + \mathbf{1} \rightarrow \mathbf{Li}\cdot\mathbf{1} + \frac{x}{2}\text{C}_8\text{H}_{18} + x\text{H}_2\text{O}$). b) Reduction potentials for oxovanadyl host lattices relative to the lithiating reagents.^[9]

Conclusion

We summarize here the main points of the present investigation and their significance for the further development of the related fields.

- 1) The synthesis of a new coordination π – π framework that contains hydrophilic and hydrophobic cavities has been described.
- 2) This study indicates that the cooperative π – π scaffolding is a powerful strategy for producing ordered materials with cavities or channels.
- 3) This study demonstrates that robust coordination polymers that contain polar channels and oxygen-rich metal centers are promising materials for a new range of applications in redox metal-ion intercalation.
- 4) The above interesting results encouraged us to throw more light on the development of lithium-ion intercalation into such polar channels of **1**, which could lead to a new cathode material for rechargeable lithium batteries as well as a new Li^+ sensitive electrode for determination of lithium ions in body fluids.

Experimental Section

Techniques: Powder XRD patterns were collected on a Siemens D-5000 diffractometer and with $\text{Cu}_{\text{K}\alpha}$ ($\lambda = 1.5408 \text{ \AA}$) radiation. ^7Li NMR spectra were recorded at 233.162 MHz (14.1 T) on a Varian Unity Inova 600 NMR spectrometer with 5.5 μs pulses, and recycle delays of 1 s. Chemical shifts are quoted in ppm relative to LiNO_3 . Infrared spectra were recorded on a Bruker Equino 55 FTIR spectrophotometer with a resolution of 4 cm^{-1} , by using samples with KBr. Thermogravimetric curves were measured on a Perkin–Elmer TGA 7lab instrument. Electrochemical experiments were performed by employing a BAS CV-50W voltammetric analyzer in a three-electrode cell with a Pt working electrode, platinum wire counter electrode, and Ag/AgCl reference electrode.

Synthesis of 1: The reaction was carried out in a 23 mL Parr Teflon-lined acid digestion bomb, heated in a Linberg/blue programmable electric furnace. A reaction mixture of V_2O_5 (0.0749 g, 1.0 mmol), $\text{H}_2\text{C}_4\text{O}_4$ (0.1708 g, 1.5 mmol), phen (0.0992 g, 0.5 mmol), CsOH (0.3 mL), and H_2O (8 mL) was sealed in a 23 mL Teflon-lined stainless autoclave, heated at 200°C for 96 h, and cooled to 70°C at 9°C h^{-1} . Orange crystals were filtered off and washed with deionized water. The yield of crystalline material was 74% (0.1224 g) based on phen, and the synthesis was highly reproducible. Energy-dispersive X-ray fluorescence analysis shows that no Cs present in the orange crystals. A sample (157.2 mg) heated by IR radiation (Mark 2 HP moisture analyzer) reveals weight loss of 2.36% below 200°C , indicating that compound **1** contains one H_2O molecule (calcd 2.7%) per formula unit. Selected IR bands: $\tilde{\nu} = 968$ (m, $\text{V}=\text{O}$), 1468 – 1600 (s, $\text{C}=\text{C}$, $\text{C}=\text{O}$), 3061 (m, $\text{C}-\text{H}$), 3538 – 3620 cm^{-1} (m, $\text{O}-\text{H}$, water). Elemental analysis calcd (%) for $\text{C}_{28}\text{H}_{20}\text{N}_4\text{O}_9\text{V}_2$: C 51.04, N 8.51, H 3.04; found: C 50.47, N 8.50, H 2.75.

Crystallography: The X-ray diffraction data were collected on a CAD4 Enraf-Nonius diffractometer with the graphite monochromated $\text{Mo}_{\text{K}\alpha}$ radiation ($\lambda = 0.71069 \text{ \AA}$) in the $\omega/2\theta$ scanning mode. Crystal size $0.12 \times 0.12 \times 0.22 \text{ mm}$, monoclinic, space group $C2/c$, $a = 20.707(3)$, $b = 9.331(2)$, $c = 17.050(5) \text{ \AA}$, $\beta = 123.85(2)$; $V = 2736(1) \text{ \AA}^3$, $Z = 4$, $F(000) = 1336$, $\rho_{\text{calcd}} = 1.598 \text{ Mg m}^{-3}$, $\mu = 7.46 \text{ cm}^{-1}$, $2\theta_{\text{max}} = 50^\circ$; 2402 unique reflections; 1537 observed reflections [$I > 2\sigma(I)$]; 235 parameters; $R_1 = 0.0351$, $wR_2(F^2) = 0.0897$, and $\text{GOF} = 0.955$; residual electron density between -0.36 and 0.27 e \AA^{-3} . Crystallographic data (excluding structure factors) for the structure reported in this paper have been deposited with the Cambridge Crystallographic Data Centre as supplementary publication no. CCDC-408643. Copies of the data can be obtained free of charge on application to CCDC, 12 Union Road, Cambridge CB21EZ, UK (fax: (+44) 1223-336-033; e-mail: deposit@ccdc.cam.ac.uk).

Lithium-ion intercalation of 1: Lithium-ion intercalation of **1** was prepared according to the reported procedures with certain modifications.^[24] All reactions were carried out under a vacuum system. A mixture of **1** (50 mg) and LiNO_3 (350 mg) was thoroughly mixed and heated at 110°C for 5 h. After dehydration, the mixed powder was cooled down to room temperature, then frozen instantly with ice bath. Upon cooling to 0°C , n -butyllithium (5 mL) was added dropwise. Over a period of 3 h the solid changed from orange to very dark black. After stirring for overnight over a water bath, the resulting dark black **Li**·**1** solid was filtered off, washed thoroughly with diethyl ether (to remove C_8H_{18}) and then with deionized water, and dried at room temperature.

Acknowledgement

This work was supported by the National Science Council of the Republic of China (NSC 89-2113-M-005-021) and the Chinese Petroleum Corporation (NSC 89-CPC-7-005-002).

- [1] J. R. Owen, *Chem. Soc. Rev.* **1997**, 26, 259–267.
- [2] P. G. Bruce, *Chem. Commun.* **1997**, 1817–1824.
- [3] M. Winter, J. O. Besenhard, M. E. Spahr, P. Novak, *Adv. Mater.* **1998**, 10, 725–763.
- [4] Y. Zhang, J. R. D. Debor, C. J. O'Connor, R. C. Haushalter, A. Clearfield, J. Zubieta, *Angew. Chem.* **1996**, 108, 1067–1069; *Angew. Chem. Int. Ed. Engl.* **1996**, 35, 989–991.
- [5] G. Chirayil, E. A. Boylan, M. Mamak, P. Y. Zavalij, M. S. Whittingham, *Chem. Commun.* **1997**, 33–34.
- [6] R. S. Prabaharan, M. S. Michael, S. Radhakrishna, C. Julien, *J. Mater. Chem.* **1997**, 7, 1791–1796.
- [7] G. Ceder, Y.-M. Chiang, D. R. Sadoway, M. K. Aydinol, Y.-I. Jang, B. Huang, *Nature* **1998**, 392, 694–696.
- [8] A. R. Armstrong, P. G. Bruce, *Nature* **1996**, 381, 499–450.
- [9] D. W. Murphy, P. A. Christian, *Science* **1979**, 205, 651–656.
- [10] M. J. Zaworotko, *Angew. Chem.* **1998**, 110, 1269–1271; *Angew. Chem. Int. Ed.* **1998**, 37, 1211–1213.
- [11] C. Janiak, *Angew. Chem.* **1997**, 109, 1499–1502; *Angew. Chem. Int. Ed. Engl.* **1997**, 36, 1431–1434.
- [12] H. Li, A. Laine, M. O'Keeffe, O. M. Yaghi, *Science* **1999**, 283, 1145–1147.
- [13] S. S.-Y. Chui, S. M. F. Lo, J. P. H. Chartmant, A. G. Orpen, I. D. Willoams, *Science* **1999**, 283, 148–150.
- [14] S.-I. Noro, S. Kitagawa, M. Kondo, K. Seki, *Angew. Chem.* **2000**, 112, 2161–2164; *Angew. Chem. Int. Ed.* **2000**, 39, 2081–2084.
- [15] M. Kondo, T. Okubo, A. Asami, S.-I. Noro, T. Yoshitomi, S. Kitagawa, T. Ishii, H. Matsuzaka, K. Seki, *Angew. Chem.* **1999**, 111, 190–193; *Angew. Chem. Int. Ed.* **1999**, 38, 140–143.
- [16] K. J. Lin, *Angew. Chem.* **1999**, 111, 2894–2897; *Angew. Chem. Int. Ed.* **1999**, 38, 2730–2731.
- [17] K. J. Lin, K. H. Lii, *Angew. Chem.* **1997**, 109, 2166–2167; *Angew. Chem. Int. Ed. Engl.* **1997**, 36, 2076–2077.
- [18] The polar environment means that the cavities or channels are enclosed by polar bonds such as $\text{C}=\text{O}$ bonds. Since the large electronegative difference between C ($\text{EN} = 2.5$) and O ($\text{EN} = 3.5$) makes each $\text{C}=\text{O}$ bond quite polar, the electron density is pulled toward the more electronegative O atoms. Hence, the lattice energy of Li^+ complexes is expected to increase, in a manner similar to crown ether molecules.
- [19] S. F. Lai, C. Y. Cheng, K. J. Lin, *Chem. Commun.* **2001**, 1082–1083.
- [20] The average $\text{V}-(\mu\text{-OH})$ bond length of $1.968(2) \text{ \AA}$ in **1** is significantly longer than that of the reported $\text{V}-(\mu\text{-O})$ bond length of 1.82 \AA .^[21]
- [21] A. Müller, F. Peters, *Chem. Rev.* **1998**, 239–271.
- [22] I. D. Brown, D. Altermatt, *Acta Crystallogr. Sect. B* **1985**, 41, 244–247.
- [23] A. Dyer, A. Molyneux, *J. Inorg. Nucl. Chem.* **1968**, 30, 829–837.
- [24] M. S. Whittingham, R. R. Chianelli, *J. Chem. Edu.* **1980**, 57, 569–574.

Received: May 21, 2001 [F3269]